Resonance Raman Spectroscopy of Discrete Silica-Supported Vanadium Oxide

Cristina Moisii, Lambertus J. van de Burgt, and A. E. Stiegman*

Department of Chemistry and Biochemistry, Florida State University, Tallahassee, Florida 32306

Received January 9, 2008. Revised Manuscript Received March 25, 2008

Vanadium oxide deposited as discrete oxovanadium groups, $[(-O)_3V{=}O]$, in transparent silica xerogels were investigated by resonance Raman spectroscopy. Spectra were collected at 351 and 257 nm excitation into two distinct absorption bands of the oxovanadium site. Three new bands associated with vibrations of the vanadium oxide site were observed at 496, 568, and 720 cm^{-1}. From these additional modes and the previously known vibrations at 1064, 1033, and 923 cm^{-1} an empirical force field was determined from which a normal-mode analysis of the primary stretching vibrations of the vanadium oxo group was carried out. This analysis indicates that for most of the observed bands the interfacial Si−O−V stretches are the primary component, and in fact, only the weak band at 923 cm^{-1} was dominated by the terminal V═O stretch. Shifts in the band positions with ^{18}O isotopic enrichment are in general agreement with the normal-mode analysis, moreover, the enrichment indicates that the bridging groups are generally quite labile to substitution.

Introduction

Vanadia deposited at the monolayer or submonolayer dimension on silica and other oxide supports is an important example of single-site heterogeneous catalysts.[1–3] These groups, which are nominally of C_{3v} site symmetry with a short terminal V═O bond and three V−O−Si linkages to the surface, are significantly more reactive than either the pure oxide or dispersed crystalline V_2O_5 deposited on the surface. While the coordination environment of the vanadium site and its chemical and catalytic properties has been largely elucidated, there are still unresolved issues related to the electronic structure of the site and its coupling with the silica surface. These issues are important in understanding the effect of a substrate on catalytic oxidation processes. For this reason, an understanding of the nature of the vibrational modes that are coupled to the surface is of considerable interest since they relate directly to the strength of the interfacial interaction. In this study we report the resonance Raman spectra of the isolated vanadium site, collected at excitation wavelengths coincident with the major electronic transients of the site. Resonance enhancement allows the observation and assignments of several new bands associated with the vanadium oxo group and analyzing the normal modes that arise from the coupling with the surface.

Experimental Section

Xerogel Synthesis. Vanadia−silica xerogel monoliths were made by a previously reported technique.[4,5] Briefly, sols were made by the slow addition of a water/isopropanol/acid (HCl) mixture to an alcoholic solution of tetramethylorthosilicate and the desired quantity of oxovanadium triisopropoxide. All solutions were ultrasonically mixed for a period of 5 min to ensure homogeneous mixing. After addition, 4 mL of the sol was placed in 1 cm styrene cuvettes, sealed, and allowed to gel. After gelation, the caps were removed and the gel was allowed to age under conditions of low humidity, which was accomplished in a closed container with saturated LiCl solutions. Typical aging-evaporation times were on the order of 3 months. The samples were then dried in a programmable furnace. They were initially ramped to 100 °C at a rate of 0.5 °C/h, where they were allowed to dry for 72 h. They were then ramped at the same rate to 500 °C, where they were maintained for 36 h. Finally, they were cooled back to room temperature over a period of 95 h.

Isotopic Labeling. ^{18}O were incorporated into the samples through a series of reduction/oxidation cycles using isotopically enriched O_2 in the oxidation step. The vanadia−silica monoliths were photoreduced under 1 atm of CO for 3 h in a quartz cell using a 200 W high-pressure mercury lamp (Oriel) with a 324 nm cutoff filter, which reduces the V^{5+} primarily to V^{3+}. At completion of the photoreduction the monolith was transferred in an inert environment to a high-pressure bomb, where it was pressurized with 125 psi of $^{18}O_2$ (Isotec, 97 atom %). Oxidation was carried out at 500 °C for a period of 12 h. Four reduction/oxidation cycles were performed on the samples to achieve the isotopic incorporation reported here. Raman spectra were collected between cycles; great care was taken to see that the samples were not exposed to ambient conditions.

Raman Spectroscopy. Raman spectra were obtained using a micro-Raman spectrograph, JY Horiba LabRam HR800, excited by one of two lasers depending on the excitation wavelength. The spectrograph uses either a holographic notch filter (for 351 and 785 nm excitation) or an edge filter (for 257 nm excitation) to couple the laser beam into the microscope (Olympus BX30) by total

* To whom correspondence should be addressed. Phone: 850-644-6605. E-mail: stiegman@chem.fsu.edu.

(1) Bond, G. C.; Tahir, S. F. *Appl. Catal.* **1991**, *71*, 1.
(2) Wachs, I. E.; Chen, Y.; Jehng, J. M.; Briand, L. E.; Tanaka, T. *Catal. Today* **2003**, *78*, 13.
(3) Weckhuysen, B. M.; Keller, D. E. *Catal. Today* **2003**, *78*, 25.
(4) Curran, M. D.; Gedris, T. E.; Stiegman, A. E.; Plett, G. A. *Chem. Mater.* **1999**, *11*, 1120.
(5) Stiegman, A. E.; Eckert, H.; Plett, G.; Kim, S. S.; Anderson, M.; Yavrouian, A. *Chem. Mater.* **1993**, *5*, 1591.

10.1021/cm800095g CCC: $40.75
Published on Web 05/21/2008

reflection. The beam is focused on the sample through a microscope objective with backscattering radiation collected by the objective. Rayleigh scattering is filtered out by the notch/edge filter with Raman scattering coupled into the spectrograph through a confocal hole. A 76 mm square grating disperses the Raman scattering onto a 1024 × 256 element open CCD detector, a Coherent I-308 argon-ion laser emitting 53 mW of power at 488 nm that was attenuated by an OD 2 neutral density filter. The power at the sample was 25 mW. The spectrograph uses a holographic notch filter to couple the laser beam into the microscope (Olympus BX30) by total reflection.

Raman spectra were collected using three different excitation wavelengths. A Coherent I300C FreD argon-ion laser operating in frequency-doubled mode supplied 45 mW excitation power at 257 nm (4 mW at the sample). The same laser operating in fundamental mode supplied 50 mW excitation power at 351 nm (5 mW at the sample). A TUIOptics (now TOPTICA Photonics) DL 100 grating-stabilized diode laser supplied 80 mW at 785 nm (6 mW at the sample). Low-power microscope objectives were used to both allow the long working distance required by the sample cell and increase the Raman signal in a semitransparent sample. Fused silica windows were used in the sample cell to collect the 785 nm excited spectra, but Raman scatter from the window became unavoidable in the ultraviolet, necessitating the use of sapphire windows to collect the 257 and 351 nm excited spectra. The sharp-featured sapphire Raman spectrum can be excluded by careful sample alignment. To maintain roughly the same spectral resolution in the different spectral regions, gratings having the appropriate line density were chosen: 3600 lines/mm for 275 nm spectra, 1800 lines/mm for 351 nm spectra, and 600 lines/mm for 785 nm spectra. The CCD detector has a quantum efficiency of 34% around 275 nm, 30% around 375 nm, and 48% around 800 nm.

Polarization ratios (I_{HV}/I_{HH}) were calculated from the integrated intensity of the peaks obtained from Raman spectra in which the scattered radiation was collected parallel (I_{HH}) and perpendicular (I_{HV}) to the polarization of the excitation beam.

Simulated Raman spectra were calculated using the Vibratz (Version 2.1) normal coordinate analysis program (Shape Software, Inc.).[6] Calculations were performed on a model structure, $(Si-O-)_3VO$, using bond lengths and angles of (V=O) =1.56 Å, (V−O) = 1.75 Å, (Si−O) = 1.65 Å, ∠(Si−O−V) = 145°, and ∠(O−Si=O) = 109.5°. The bandwidths plotted in the simulation were adjusted to bring them into agreement with the experimentally observed bandwidth.

Results and Discussion

The electronic spectrum of a 0.005 mol % vanadia−silica xerogel is shown in Figure 1. The spectrum shows no measurable absorbance until about 380 nm, where a band is observed with $\lambda_{max} \approx 330$ nm and an extinction coefficient of 5×10^2. To higher energy, a more intense transition is observed with a $\lambda_{max} \approx 235$ nm ($\epsilon = 5.2 \times 10^3$).[7,8] While these broad bands are undoubtedly composed of more than one electronic transition, emission polarization anisotropy studies indicate that these two spectral regions contain transitions of differing symmetries. Resonance Raman spectra were collected with excitation into these two bands at 351

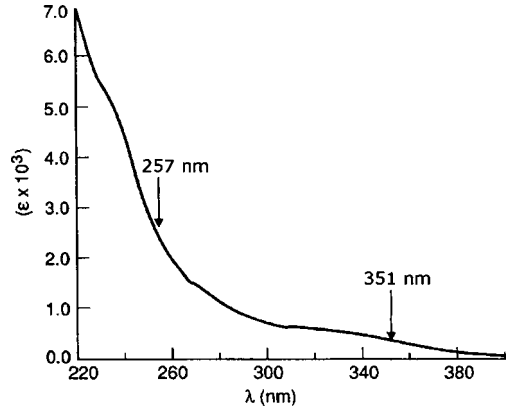

Figure 1. UV−vis spectrum of a 0.005 mol % vanadium−silica xerogel indicating the excitation wavelengths used for resonance Raman spectroscopy (note: the silica background spectrum has been subtracted).

and 257 nm. Notably, emission from the lowest excited state is centered in the green at ∼550 nm with an onset at ∼375 nm, which is close to the zero-point energy. The spectral region between the onset of emission and the first observable electronic transition contains very weak absorptions, which are observable in the emission excitation spectrum. While it would be desirable to obtain resonance Raman in this region to probe the vibration coupled to the lowest excited state, the extremely low extinction coefficients and interference from the emission effectively preclude it.

Raman spectra collected off-resonance at 785 nm and on-resonance at 351 and 257 nm are shown in Figure 2. A comparison of the two spectra collected on-resonance with the nonresonance spectrum shows that resonance enhancement is observed for certain modes assigned to the vanadium site, and the appearance of bands not previously observed due to spectral overlap with the silica features are also observed. Excitation at 351 nm (Figure 2b), into the weaker of the two absorption bands, produces an apparent enhancement, relative to the silica features, of the intense band at 1033 cm^{-1}, which is historically assigned to the terminal V=O stretch. Also enhanced, concomitant with the terminal V=O stretch, is the band appearing as a shoulder at ∼1060 cm^{-1}. This band is also observed in the nonresonance spectra of the vanadium site, and in our previous analysis, we suggested that its origin was from an underlying mode largely involving silica stretches at the interface with the vanadium.[9] The band appearing at ∼923 cm^{-1}, which is highly convoluted with the Si−OH band at 976 cm^{-1}, is more easily resolved at this excitation, which suggests modest resonance enhancement. Also apparent is a sharp band at 487 cm^{-1}, which is observed above the strong silica features.

Excitation into the intense high-energy band at 257 nm results in strong resonance enhancement of several of the vibrational modes. The band at 1033 cm^{-1} appears to be enhanced as much as it was at 351 excitation; however, the most striking enhancement observed is that of the high-energy shoulder at ∼1060 cm^{-1}, which becomes a well-resolved peak at 1064 cm^{-1}. This mode is clearly very strongly coupled to the high-energy electronic transition. The

(6) www.shapesoft.com.
(7) Tran, K.; Hanninglee, M. A.; Biswas, A.; Stiegman, A. E.; Scott, G. W. *J. Am. Chem. Soc.* **1995**, *117*, 2618.
(8) Tran, K.; Stiegman, A. E.; Scott, G. W. *Inorg. Chim. Acta* **1996**, *243*, 185.
(9) Moisii, C.; Curran, M. D.; van de Burgt, L. J.; Stiegman, A. E. *J. Mater. Chem.* **2005**, *15*, 3519.

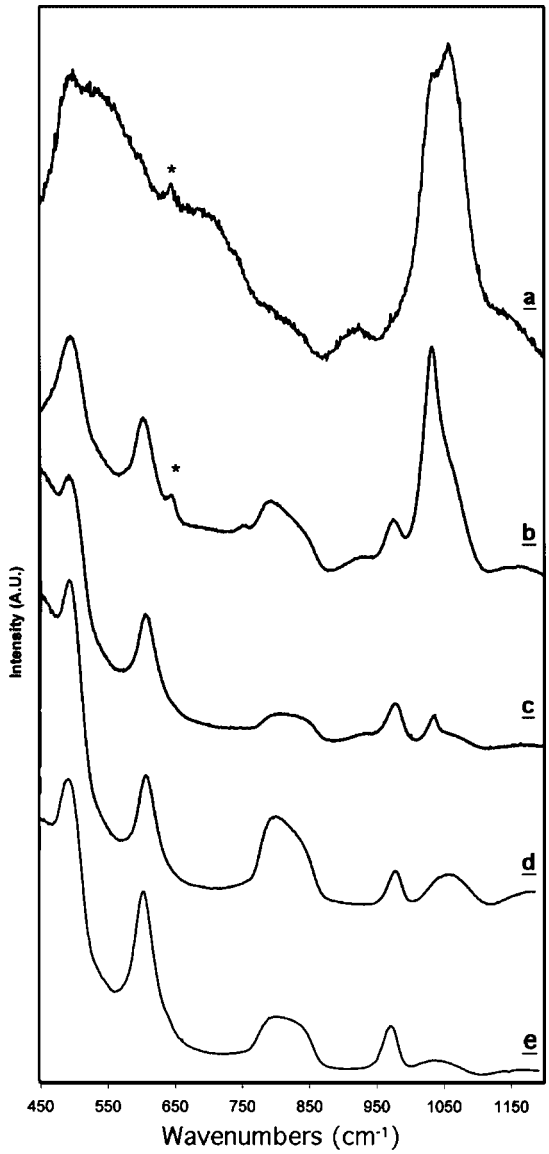

Figure 2. Raman spectra of a 0.5 mol % vanadium−silica xerogel collected on-resonance with (a) 257 and (b) 351 nm excitation and (c) off-resonance with 785 nm excitation, and Raman spectra of pure silica control samples collected at (d) 351 and (e) 257 nm (asterisk (*) indicates contribution from sapphire optical windows).

band at ∼923 cm^{-1} also appears to be resonance enhanced, but this is far less pronounced and may simply reflect the expected nonresonance intensity increase that accompanies higher frequency excitation. Also apparent in the spectrum are two broad highly convoluted bands albeit with resolved peaks at ∼570 and ∼720 cm^{-1}.

More details of the enhanced modes are obtained by deconvolution of the spectra, which is shown in Figure 3. In general, deconvolution algorithms can over- or underdetermine the number of bands contributing to a spectrum, thereby producing spurious results. As a matter of course we generally discount deconvolution results that generate peaks not directly observed in the spectrum or are known to be there for other reasons. In our previous study the nonresonance Raman spectrum of a 0.5 mol % sample was deconvoluted cleanly with no spurious peaks generated.[9] The modes associated with the vanadium were found to be at 1033 and 923 cm^{-1}, the 1060 shoulder is weak, and it was not resolved from the TO antisymmetric silica stretch at 1066 cm^{-1}.[9] The rest of the peaks are silica modes including the Si−OH stretch at 977 cm^{-1} and the sharp D_2 and D_1 defect ring modes at 607 and 498 cm^{-1}, respectively. Deconvolution of the resonance Raman spectrum collected at 351 nm excitation is shown in Figure 3a. The high-frequency modes associated with the vanadium are cleanly deconvoluted at 1064, 1033, and 923 cm^{-1}, consistent with their increased intensity due to resonance enhancement. In the low-frequency regime several things are notable. One is that there are two broad intense bands generated by the deconvolution algorithm at 713 and 574 cm^{-1}. These bands are not directly resolved in the spectrum but are generated by the software to account for the increase in intensity that is evident in this region when compared to the nonresonance spectrum. Finally, there is a sharp intense peak at 496 cm^{-1} that in the nonresonance spectrum is obscured by the D_1 silica ring defect mode at 498 cm^{-1} and appears only at high concentrations of vanadium (∼10%). Due to its strong enhancement at 351 nm excitation it becomes observable at low vanadium concentration, and as a result, it is clear that it is an intrinsic band of the isolated vanadium oxo species. Deconvolution of the resonance Raman spectrum collected with 257 nm excitation is shown in Figure 3b. The signal-to-noise is generally poorer due to self-absorption at this wavelength. The high-frequency region shows the known vanadium oxo group bands properly deconvoluted and clearly shows the strong resonance enhancement of the 1064 cm^{-1} mode relative to the 1033 band. The 923 cm^{-1} band is better resolved at 257 nm excitation and placed by the deconvolution routine at a frequency of 912 cm^{-1}. The Si−OH band, which is no longer resolved due to spectral congestion, is also generated by the deconvolution routine. In the low-frequency region bands at 568, 699, and 487 cm^{-1} are observed as resolved peaks in the spectrum. Notably, these are quite close to the modes generated in the deconvolution of the 351 nm resonance spectra. Since pure silica controls excited at this wavelength show no bands in this region (Figure 2d and 2e) they must be associated with the vanadium oxo group and are now observed over the silica background due to resonance enhancement.

Empirical Analysis of the Primary Stretching Modes

A total of six bands associated with the vanadium oxo group are resolved through Raman spectroscopy. They are the previously reported bands at 1064, 1033, and 923 cm^{-1} observable in nonresonance Raman spectroscopy and bands at 699, 568, and 496 cm^{-1} observable due to resonance enhancement. For analysis of these modes an eight-atom model system was used with the V═O group connected to three silicon atoms at the surface while maintaining an idealized C_{3v} point group, i.e., $(Si-O-)_3V{=}O$. For this model there will be 18 vibrational modes of which 17 will be observable by Raman (there is an A_2 mode that is inactive). Of the normal modes 7 will be stretching modes ($3A_1$ and 2E) and 10 will be bending modes ($2A_1$ and 4E); taking into account degeneracy there will be 5 stretching and 6 bending modes that are potentially observable. In the Raman spectrum, the three high-energy modes at 923, 1033,

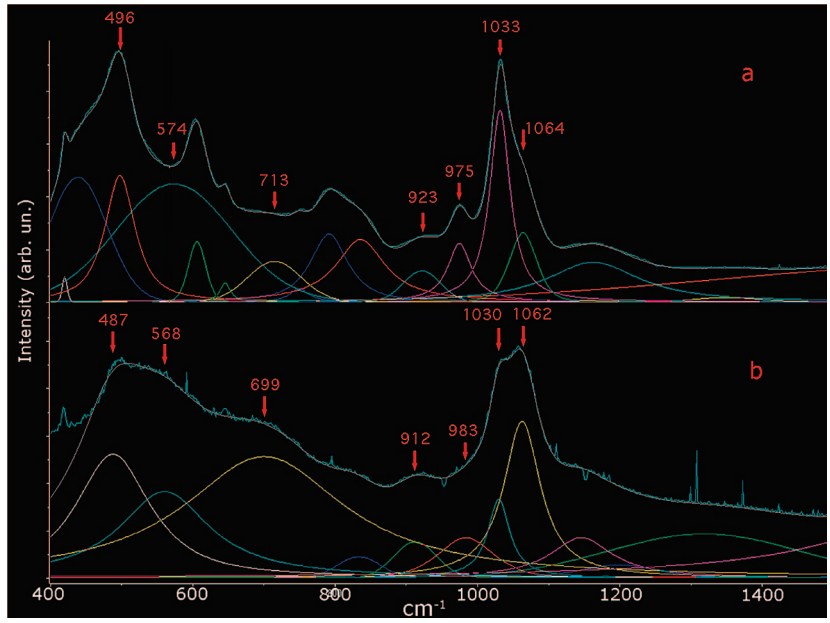

Figure 3. Deconvolution analysis of resonance Raman spectra of 0.5 mol % vanadium−silica xerogel collected with (a) 351 and (b) 257 nm excitation.

Table 1

	Raman stretching bands (cm^{-1})					force constants (mdynes/Å)				
	E	A_1	A_1	E	A_1	*f*(V=O)	*f*(V−O)	*f*(Si−O)	*f*(V−O,V=O)	*f*(V−O,V−O)
obsd	1064	1033	923	568	496	6.28				
calcd (est. central f.c.)	1050	1031	937	570	474	6.28	4.5	4.5		
calcd (refined central f.c.)	1065	1032	923	568	484	6.28	5.47	3.84		
calcd (refined central, off-diagonal f.c.)	1064	1033	923	568	496	5.74	5.20	3.84	0.300	0.144

and 1064 cm^{-1} are most likely stretching fundamentals because of their energy and intensity. The low-frequency modes at 723, 568, and 496 cm^{-1} are somewhat more difficult to assign as they may be either bending or stretching modes. Moreover, while peaks are resolved at these frequencies through direct observation and deconvolution there is a great deal of spectral congestion in this region due to the enhanced vanadium oxo bands and the intense silica modes that are present. As such, the peaks observed likely result from several overlapping bands, which means they cannot necessarily be assigned to a single mode. A likely exception to this is the 496 cm^{-1} band, which is quite sharp and intense in the resonance Raman collected at 351 nm excitation.

Initial analysis of observed vanadium oxo modes was carried out using a central force approximation utilizing only the diagonal stretching force constants. While crude, the central force approximation works well for oxide materials because the diagonal force constants are usually an order of magnitude or more larger than the bending or off-diagonal stretching forces. In particular, this approximation was used by Sen and Thorpe and, subsequently, by Galeener to successfully analyze the vibrational spectra of amorphous silica.[10–12] As such, it should work well within limits for the vanadium oxo system, particularly for the high-frequency stretching modes. Initial estimates of the diagonal stretching force constants were taken from the literature. In particular, the force constant of the Si−O bond was taken from the studies by Galeener on amorphous silica, which was estimated at 4.5 mdyn $Å^{-1}$; estimates for the V=O and V−O force constants were approximated from the Mn=O and Mn−F force constants, which were determined empirically to be 6.4 and 4.5 mdyn $Å^{-1}$, respectively, by Reisfeld et al. for MnO_3F.[10,13] Initial calculation of the spectra using these constants produced five modes at 474, 570, 937, 1031, and 1050 cm^{-1}. In spite of the crudeness of the force constant estimates, the bands produced agree surprisingly well with those observed in the resonance Raman spectra (Table 1). In particular, it reproduces well the known high-frequency stretching modes as well as two of the three new modes observed due to resonance enhancement. The mode at ~700 cm^{-1} is not predicted by the theory, presumably because it is a bending mode. Refinement of the three central force constants was carried out by iterative least squares to bring the predicted transition energies into better agreement with the bands observed in the spectra. Since the low-frequency region of the spectrum (<700 cm^{-1}) will contain both bending and stretching modes it is difficult to be sure whether the observed bands are stretching or bending modes or of their symmetry. In the iterative least-squares algorithm used, incorrect assignment of the modes is likely to cause the refinement to fail. For this reason the refinement was initially carried out using only the three high-frequency modes whose assignments are most firm. The force constants resulting from

(10) Galeener, F. L. *Phys. Rev. B* **1979**, *19*, 4292.
(11) Galeener, F. L.; Leadbetter, A. J.; Strongfellow, M. W. *Phys. Rev. B* **1983**, *27*, 1052.
(12) Sen, P. N.; Thorpe, M. F. *Phys. Rev. B* **1977**, *15*, 4030.
(13) Reisfeld, M. J.; Asprey, L. B.; Matwiyof, N. *Spectrochim. Acta A* **1971**, *A 27*, 765.

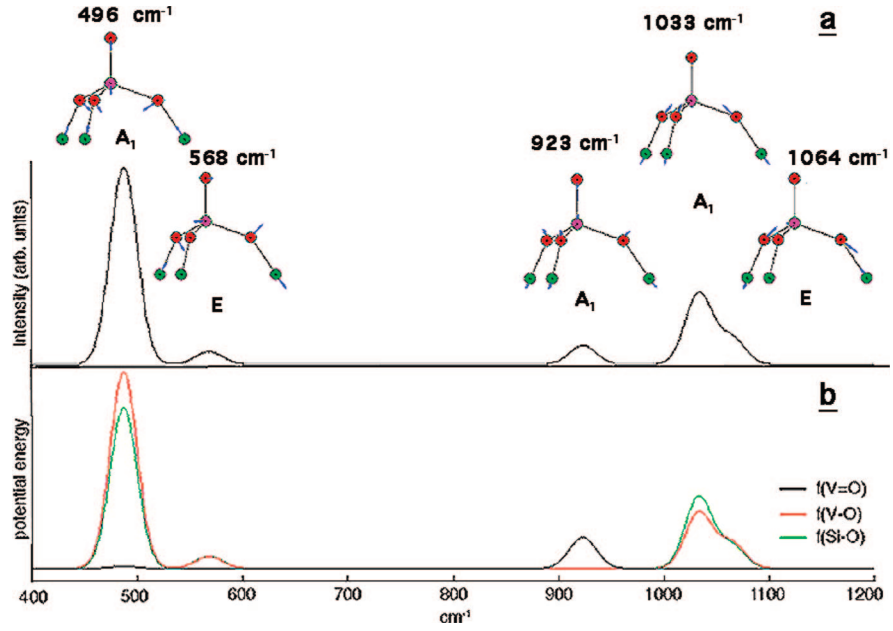

Figure 4. (a) Raman spectrum simulated using the calculated empirical force field and the normal modes associated with the bands generated in the simulation, and (b) the potential-energy distribution showing the contribution of each of the diagonal stretching force constants to the spectrum.

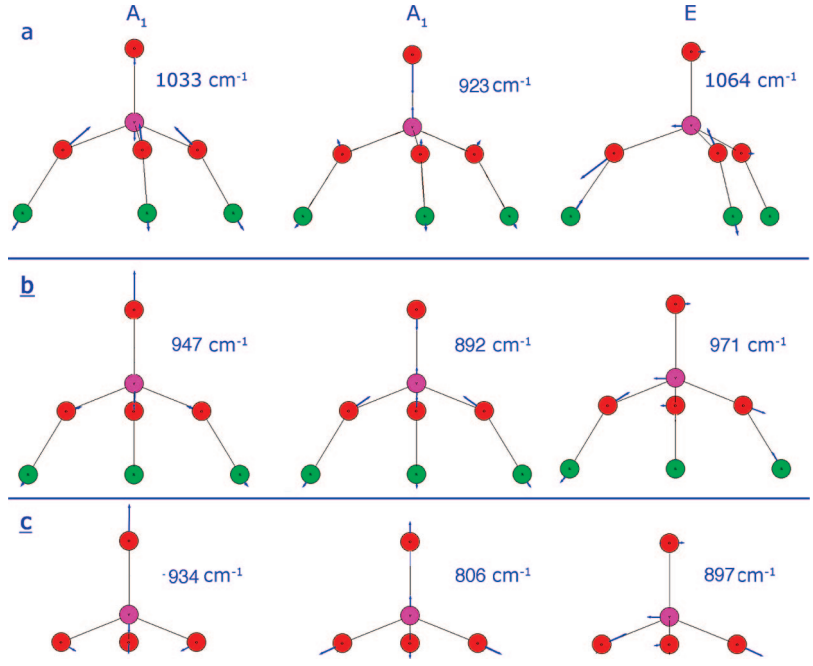

Figure 5. Atomic motion of the three high-energy stretching modes of the silica-supported oxovanadium group as a function of the strength of interaction with the surface as controlled by an *f*(Si−O) force constant of (a) 3.8, (b) 2.0, and (c) 0.00 mdynes/Å.

this assignment, shown in Table 1, are reasonable in magnitude, particularly in view of the simplicity of the force field, and correspond well to the empirically determined stretching force constants for small molecule analogues containing similar bonds. As would be expected, the three high-frequency modes now agree almost exactly, but more importantly, the position of the two low-frequency modes are predicted to within 10 cm^{-1} of their observed frequencies. This supports the assignment of these modes to stretches and suggests that all of the stretching modes for the silica-bound vanadium oxide have been resolved. By including all of the bands the empirical force field can be expanded to include two off-diagonal stretching interaction terms, specifically *f*(V−O,V═O) and *f*(V−O,V−O). An initial seed value of 0.40 mdyn $Å^{-1}$ was used for both off-diagonal terms. All five of the force constants were then refined against the five stretching frequencies. The final values of the force constants are given in Table 1, while the simulated spectrum obtained from the calculations is shown in Figure 4a. Notably, attempts made to simulate the ∼700 cm^{-1} band through addition of a bending force constant were not successful.

Using the empirical force field the normal modes associated with the primary stretching bands could be analyzed, the results of which are shown in Figures 4a and 5a. The well-studied 1033 cm^{-1} band, which is typically referred to as the "V═O" stretching mode in the group frequency

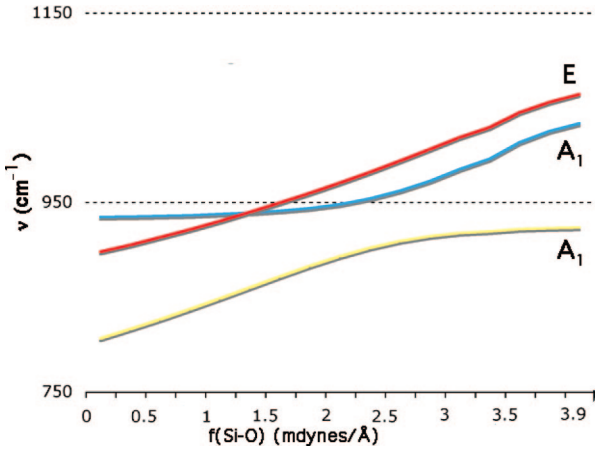

Figure 6. Systematic change in the three high-energy stretching modes as the $(-O)_3V{=}O$ group bonds to the silica surface simulated by varying f(Si−O) from zero to it is empirically determined value for the bound group (all other force constants were held fixed).

approximation, and the 923 cm^{-1} band, which was previously assigned by us to a Si−O−V stretching mode, are both totally symmetric stretches.[9,14] The normal-mode analysis indicates that both are composed of concerted stretching of the V═O bond coupled to stretching of the bridging Si−O−V bonds. In the 1033 cm^{-1} mode the dominant stretch is the Si−O−V bridge, which is opposed by the V═O atomic motion with both of those atoms moving in the same direction (Figure 5a). In the 923 cm^{-1} mode the V═O stretch is out of phase with the Si−O stretch and the dominant atomic motion. The calculated contribution of each of the three central force constants to the potential energy of each mode is shown in Figure 4b. As can be seen, the V═O force constant actually makes the largest contribution to the 923 cm^{-1} band, while for the 1033 cm^{-1} mode f(Si−O) and f(V−O) both make larger contributions to the overall potential energy than does f(V═O). Essentially, to the extent that group stretching frequencies apply, the "V═O" stretch more appropriately describes the 923 cm^{-1} band than the 1033 cm^{-1} band. The 1064 cm^{-1} mode is an E symmetry mode that involves out-of-phase movement of the bridging atoms. It involves little contribution from the V═O and is, in effect, the mode most accurately described as the bridging stretch, though, notably, all three involve some degree of contribution from the Si−O−V bridge. This is reasonable since the force constants for Si−O and M−O are usually close in value. Finally, the bands at 568 and 496 cm^{-1}, which are observed due to resonance enhancement, are of E and A_1 symmetry, respectively. The normal-mode analysis of these bands (Figure 4a) indicates that both are stretching modes involving primarily the Si−O−V bridge. The A_1 mode involves an in-phase motion of the V and terminal O, which is opposed by the Si and bridging O atom. The E mode is similar to the 1064 cm^{-1} E mode in that the V and terminal O are moving out of phase with each other in parallel to the surface.

The evolution of the normal modes as the vanadium oxo group is attached to the surface is of interest in understanding the effect of the support on the catalytic site. Figure 6 shows the changes in the normal modes and their frequencies as the f(Si−O) force constant goes from zero, for an unattached $O_3V{=}O$ unit, to a value of 3.9 mdynes/Å for the surface-bound species with all other force constants held constant in the analysis. For the $O_3V{=}O$ species the stretching modes are at 934 (A_1), 897 (E), and 806 (A_1) cm^{-1} with the 934 cm^{-1} band being primarily a V═O stretch. Notably, the three stretching modes for $F_3V{=}O$ appear in the same order at 1057, 806, and 721 cm^{-1} which, given the difference in the molecular species and crudeness of the approximation, is reasonably close in value.[15] As the interaction force constant, f(Si−O), between the silicon on the surface to the $O_3V{=}O$ group increases, the frequencies of the modes also increase with that of the E mode doing so more rapidly until it surpasses the two A_1 modes at f(Si−O) ≈ 1.25 mdynes/Å . The two A_1 modes approach each other but never cross and then diverge again at f(Si−O) ≈ 2.25 mdynes/Å. Importantly, Figure 6 shows that as the f(Si−O) force constant gets larger, the frequencies begin to plateau somewhat and the frequency varies slowly with the force constant so that in the range where the interfacial force constant approaches realistic values (≳3.5 mdynes/Å) there is only a modest shift in the frequency for all of the bands. For example, between f(Si−O) = 3.5 and 3.9 the frequency of the high-energy A_1 modes varies between 1012 and 1033 cm^{-1}. This explains the experimental observations that isolated vanadium sites on various pure and mixed oxide substrates show only modest variations in the primary 1033 cm^{-1} A_1 stretching mode. [16–19]

The evolution of the normal modes as a function of the f(Si−O) force constant is shown in Figure 5b and 5c. It can be seen that as the coupling to the silica surface becomes stronger the motion of the V═O atoms changes direction to compensate for coupling with the surface. The 923 cm^{-1} A_1 band in free $O_3V{=}O$, which ultimately correlates to the 1033 cm^{-1} A_1 modes at the silica surface, is largely dominated by opposite motion of the vanadium and terminal oxygen with a compensatory bending of the V−O single bonds (Figure 5a). As the Si−O force becomes stronger the V and O atoms of the V═O group begin to move in phase and opposed to the Si−O stretch ultimately. The other A_1 stretch at 806 cm^{-1} in the free molecule, which correlates to the 923 cm^{-1} band at the surface, is largely a stretch along the V−O bond (Figure 5c) that is compensated by in-phase motion of the V and terminal O atoms. As the Si−O force constant becomes stronger the V−O stretch becomes an out-of-phase Si−O motion with the terminal oxygen moving against it. At the surface this mode is largely the V═O stretch though, as stated, all involve motion of the Si−O−V bridge. It is reasonable that the highest energy modes at the surface should largely involve Si−O−V motion since the Si−O and V−O force constants are large and there are three bonds of this type. Overall, this analysis clearly indicates that while the group vibration descriptions can be extremely useful, they

(14) Went, G. T.; Oyama, S. T.; Bell, A. T. *J. Phys. Chem.* **1990**, *94*, 4240.
(15) Selig, H.; Claassen, H. H. *J. Chem. Phys.* **1966**, *44*, 1404.
(16) Ross-Medgaarden, E. I.; Wachs, I. E. *J. Phys. Chem. C* **2007**, *111*, 15089.
(17) Gao, X. T.; Fierro, J. L. G.; Wachs, I. E. *Langmuir* **1999**, *15*, 3169.
(18) Gao, X. T.; Bare, S. R.; Fierro, J. L. G.; Wachs, I. E. *J. Phys. Chem. B* **1999**, *103*, 618.
(19) Wachs, I. E. *Catal. Today* **1996**, *27*, 437.

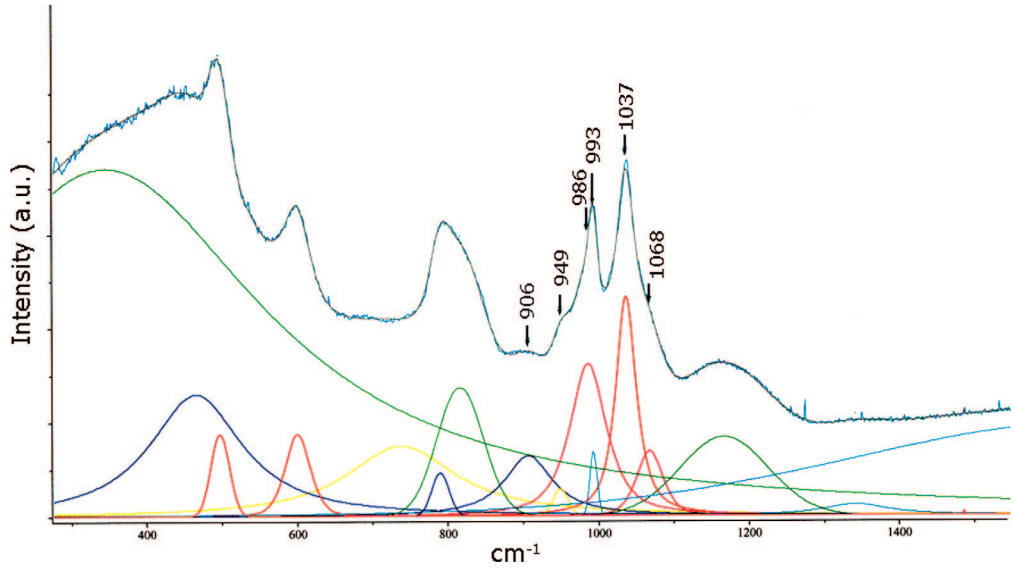

Figure 7. Deconvolution analysis of resonance Raman spectra of 0.5 mol % vanadium−silica xerogel after ^{18}O isotopic substitution collected at 351 nm excitation.

fall well short of an accurate description of the vibration modes present for surface-bound groups. Moreover, it also indicates that the nature of the surface is likely to have a profound impact on the positions of the highest energy and most intense (i.e., most readily observed) bands. In fact, the position of the highest energy E and A_1 bands or, alternatively, difference in energy between the two A_1 bands is likely to serve as a good indicator of the strength of the coupling of the vanadium site to the surface. Notably, our conclusions agree completely with that drawn previously by Magg et al. in their very careful density functional analysis of the supported vanadium site.[20]

To further understand the normal modes for the system, a comparison of the effects of ^{18}O isotopic labeling of the coordination sphere of the vanadium on the resonance-enhanced spectrum was carried out. As in our previous study, ^{18}O was incorporated into the coordination sphere of the vanadium through photochemical reduction of the vanadium in a CO atmosphere followed by thermal reoxidation under 125 psi of enriched oxygen at 500 °C.[9] The reduction−oxidation process was repeated until only minimal changes were observed in the Raman spectrum. The resonance Raman spectra at 351 nm excitation of the isotopically substituted 0.5 mol % vanadia materials is shown in Figure 7. Unfortunately, the presence of a fluorescent background in the UV after the isotopic substitution process made it impossible to collect spectra at 257 nm. Attempts to circumvent this by use of H_2 as a thermal reductant were similarly unsuccessful.

The most obvious change in the spectrum is the appearance of a sharp band at 991 cm^{-1}, which has traditionally been assigned as a 42 cm^{-1} isotopic shift of the V=O stretching mode due to ^{18}O substitution of the terminal oxo group (Figure 7).[14] The close agreement of this shift to that predicted by a diatomic oscillator approximation of the V=O stretch has caused it to be used to support the spectroscopic assignment.[9,21] The spectrum, deconvoluted into its constituent peaks, is shown in Figure 7. The deconvolution suggests that the 991 cm^{-1} peak is actually comprised of a large broad peak at 986 cm^{-1} convoluted with a very small sharp peak at 993 cm^{-1}. Since neither of these appear directly in the spectrum the validity of this decomposition is uncertain. The symmetric stretch at ~923 cm^{-1} shifts with substitution with the magnitude of the shift being large enough that it is resolved as a peak in the spectrum at 906 cm^{-1} and also appears unambiguously in the deconvolution. Notably, due to resonance enhancement this peak is much better resolved than it was in our prior study.[9] The deconvolution also shows a weak band at 949 cm^{-1}, which is the known position of the 975 cm^{-1} Si−OH stretch upon ^{18}O substitution.[22] It is clear from the spectrum that complete ^{18}O labeling was not attained as evidenced by the intensity remaining at 1033 cm^{-1} arising from nonenriched groups still remaining in the matrix. The obvious shoulder at 1064 cm^{-1} in the ^{16}O samples is not evident in the spectrum due to its lower intensity but is accurately placed there in the deconvolution. The ratio of the 1033 and 1064 cm^{-1} peak areas, taken from the deconvolution, before and after ^{18}O labeling have values of 0.25 and 0.21, respectively, which suggests that about one-fourth of the vanadium oxo sites contain no ^{18}O labeling. This means that the spectral bands resulting from isotopic substitution within the coordination sphere of the vanadium will be complex due to the differing degrees of isotopic substitution. Predictions of the band positions of the primary high-frequency stretching modes resulting from various degrees of ^{18}O substitution are listed in Table 2. Several general conclusions about the effect of ^{18}O labeling can be drawn from the predictions. Isotopic substitution of the bridging oxygens are predicted to give large isotopic shifts to the 1033 and 1064 cm^{-1} high-frequency modes, while

(20) Magg, N.; Immaraporn, B.; Giorgi, J. B.; Schroeder, T.; Baumer, M.; Dobler, J.; Wu, Z.; Kondratenko, E.; Cherian, M.; Baerns, M.; Stair, P.; Sauer, J.; Freund, H. J. *J. Catal.* **2004**, *226*, 88.

(21) Weckhuysen, B. M.; Jehng, J. M.; Wachs, I. E. *J. Phys. Chem. B* **2000**, *104*, 7382.

(22) Galeener, F. L.; Mikkelsen, J. C. *Phys. Rev. B* **1981**, *23*, 5527.

Table 2. Observed and Calculated Vibrational Frequencies (cm^{-1}) for ^{16}O and ^{18}O Labeling of Oxovanadium on Silica

obsd			
^{16}O	1064	1033	923
^{18}O	1068	991	906
	1037		
calcd			
$(^{16}O)_2(^{18}O)V{=}O$	1047	1017	922
$(^{16}O)(^{18}O)_2V{=}O$	1030	1001	921
$(^{18}O)_3V{=}O$	1015	986	919
$(O)_3V{=}O^{18}$	1064	1033	883
$(^{16}O)_2(^{18}O)V{=}^{18}O$	1047	1016	882
$(^{16}O)(^{18}O)_2V{=}^{18}O$	1030	999	882
$(^{18}O)_3V{=}^{18}O$	1015	984	881

labeling of the terminal oxygen, $V{=}^{18}O$, is predicted to have little effect on their positions. Conversely, the 923 cm^{-1} band is predicted to be strongly affected by terminal substitution, consistent with that mode being dominated by the V═O force constant. It should be noted that the predicted band shifts would be somewhat different if a more complete force field was used that coupled in more off-diagonal terms (e.g., stretching with bending modes). For the primary stretching modes, however, the empirical force field derived here should be a reasonable approximation.

The magnitude of the isotopic shift predicted from the central force approximation for the 1033 cm^{-1} A_1 band is consistent with experimental observation. As shown in Table 2, the predicted frequencies, for the higher degrees of substitution, generally fall between 984 and 999 cm^{-1}, suggesting that the 991 cm^{-1} peak found in the ^{18}O spectrum represents a weighted average of the frequency distribution among these substituted species. The broadness of the underlying peaks generated by the deconvolution algorithm is consistent with this interpretation. Notably, the very close agreement of the observed peak to the energy predicted for complete bridging oxygen substitution, suggesting that the bridging bonds must be quite active in the reduction−oxidation sequence used in the isotopic substitution process. The A_1 mode at 923 cm^{-1} shifts to 906 cm^{-1}, where it is observed as a resolved peak in the spectrum. This mode is predicted to shift to ∼881 cm^{-1} in the empirical approximation with complete labeling. The broadness of the band as calculated by the deconvolution suggests that it is composed of contributions from different degrees of substitution, including the residual ^{16}O peaks at 923 cm^{-1}. Moreover, it suggests that the terminal V═O group is not extraordinarily reactive to substitution in the redox process, and in fact, the large isotopic shifts in the 1033 cm^{-1} mode which is dominated by the Si−O−V linkage and the modest shift of the V═O dominated 923 cm^{-1} band suggests that the substitutional lability of the oxygens in the coordination sphere is approximately statistical or even favors the linking oxygens. This result strongly supports a similar suggestion put forth previously by Wachs and others.[3] Finally, the band resulting from the isotopic shift of the 1064 cm^{-1} band is not directly resolved in the spectrum. It is predicted to shift to ∼1015 cm^{-1} due primarily to bridging oxygen substitution, which places it within the envelope of bands associated with the isotopically substituted A_1 mode. Taken together, the results of the isotopic substitution are in general agreement with the predictions from the empirical analysis, although the effect of incomplete substitution and the high degree of spectral congestion leaves some band positions ambiguous. The most important conclusion to be drawn from the isotopic substitution study is the importance of the bridging oxygen linkage to the majority of observed bands and that, with one exception, out-of-phase motion of the terminal V and O atoms are not a major contributor to the modes. In our previous study we argued, based on the observation that the 42 cm^{-1} isotopic shift of the 1033 cm^{-1} was in such close agreement to the diatomic oscillator approximation, that it acted as an isolated V═O oscillator and was uncoupled from the substrate.[9] Considering the current analysis our prior argument is clearly incorrect.

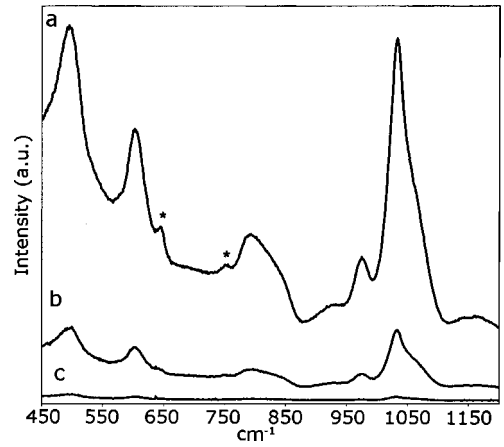

Figure 8. Resonance Raman spectrum collected at 351 nm excitation of a 0.5 mol % vanadia−silica xerogel collected (a) unpolarized and (b) parallel and (c) perpendicular polarized (asterisk (*) indicates contribution from sapphire optical windows).

As seen by comparing the spectra in Figure 2, there are excitation wavelength-dependent differences in the modes that are resonance enhanced. In particular, most of the major vanadium oxo modes appear to be enhanced relative to the silica background; however, the 1064 cm^{-1} band is strongly enhanced at 257 nm, while the 1033 cm^{-1} band is preferentially enhanced at 351 nm. The coupling of a particular vibrational mode to specific optical transitions is described theoretically by the Kramers−Heisenberg relationship.[23] The bands excited at 351 and 257 nm laser lines have large extinction coefficients, suggestive of fully allowed transitions. The parallel and perpendicular polarized spectra of a 0.5 mol % vanadium sample under resonance-enhanced excitation at 351 nm is shown in Figure 8. All of the peaks associated with the vanadium are totally symmetric with polarization ratios ≪3/4.[24] Taken together, this suggests that the resonance-enhanced modes are all A term, associated with fully allowed transitions coupled to totally symmetric modes. In our analysis we imposed a C_{3v} site symmetry on the model used, which produces both totally symmetric A_1 modes to which the 1033 and 923 cm^{-1} bands are assigned and antisymmetric E modes to which the 1064 cm^{-1} is assigned. The polarization studies and observed resonance enhance-

(23) Abello, L.; Husson, E.; Repelin, Y.; Lucazeau, G. *Spectrochim. Acta, Part a: Mol. Biomol. Spectrosc.* **1983**, *39*, 641.
(24) Long, D. A. *Raman Spectroscopy*, 1st ed.; McGraw-Hill: London, 1977.

ment indicate that these symmetry labels do not apply to the real system. This is expected since the majority of the modes involve atomic motion of the Si−O−V linkage. This interfacial region will deviate dramatically from the idealized C_{3v} site symmetry, causing the E modes to split into two A modes as the symmetry drops to C_1. Breaking the degeneracy of the E modes probably accounts for the broadness of the 1064 cm^{-1} feature at 257 nm excitation and the fact that no clear band is observed with isotopic substitution since there will be differences in how each component of the E mode is affected by ^{18}O enrichment. Notably, other metals doped into silica glasses do show polarization effects that can be used to differentiate vibrational modes. In particular, tetrahedral Ti(IV) sites in silica show strong polarization of the band at ~1100 cm^{-1} and no polarization of the band at ~960 cm^{-1}.[25,26] The lack of polarization of the ~960 cm^{-1} transition indicates that it is an antisymmetric mode; however, it may also suggest that it is a mode not strongly coupled to the silica network where the symmetry would be broken. In recent studies of Cr(VI) doped into silica we observed evidence, albeit weak, of a nonpolarized band that was consistent with the antisymmetric terminal $Cr(=O)_2$ stretching mode as calculated by Dines et al.[27] This is reasonable since the terminal modes are not likely to experience a significant reduction in symmetry as a function of the silica network. In general, this suggests that for d^0 metals bound to a surface the loss of symmetry at the site coupled with the fact that the electronic spectrum is dominated by intense LMCT bands suggest that A-term enhancement in the resonance Raman spectrum will be common and that many modes associated with the site are likely to be observed.

Conclusions

Collection of resonance Raman spectra of silica-supported vanadium oxo sites has allowed the observation and assignment of several new vibrational bands associated with the site. From these additional modes an empirical force field originating from a central force approximation could be determined. A normal-mode analysis of the primary stretching modes of the vanadium oxo group was carried out using this force field. This analysis indicates that for most of the observed bands the interfacial Si−O−V stretches are an extremely important component to the mode, and in fact, only the weak band at 923 cm^{-1} was dominated by the terminal V=O stretch. Shifts in the band positions with ^{18}O isotopic enrichment are in general agreement with the normal-mode analysis; moreover, since the enrichment is carried out through a redox process it indicates that the bridging modes are generally quite labile to substitution.

Acknowledgment. Funding was provided by the Air Force Office of Scientific Research through MURI 1606U81. We thank Israel Wachs for helpful discussions and for critical reading of an early version of this manuscript.

CM800095G

(25) Knight, D. S.; Pantano, C. G.; White, W. B. *Mater. Lett.* **1989**, *8*, 156.
(26) Soult, A. S.; Carter, D. F.; Schreiber, H. D.; van de Burgt, L. J.; Stiegman, A. E. *J. Phys. Chem. B* **2002**, *106*, 9266.
(27) Dines, T. J.; Inglis, S. *Phys. Chem. Chem. Phys.* **2003**, *5*, 1320.